Research on Engineering Structures & Materials
www.jresm.org
Research Group

Research Article

Optimized Al2011 hybrid composites reinforced with nano TiC and MoS_2 for enhanced mechanical and tribological performance

U Pradeep Kumar [1,a], Rukmangadha P [1,b], Mallaradhya H M [*,2,c]

[1]*SJC Institute of Technology, (Autonoumous), Affilatied to VTU Belgavi, Karanataka, India*
[2]*Ramaiah University of Applied Sciences, India*

Article Info

Article History:

Received 11 Aug 2025
Accepted 18 Jan 2026

Keywords:

Al2011 alloy hybrid composites;
Nano TiC;
Molybdenum disulfide;
Stir casting;
Mechanical properties;
Wear resistance;
Tribological behavior;
Microstructural analysis;
Solid lubricants;
Nano-reinforcement

Abstract

Hybrid metal matrix composites (HMMCs) are designed with the increased demand of light weight, strong and wear resistant materials in automotive and aerospace industry and structural fields. This paper reports the preparation and full characterization of Al2011-based HMMCs reinforced by different weight percent (2-10 wt%) of nano Titanium Carbide (TiC), and of a fixed composition of 4 wt% of nano Molybdenum Disulfide (MoS2) prepared by stir casting. Nano TiC with its mechanical strength and boost in load-carrying strength was added, and MoS_2 was added as a solid lubricant to improve the tribology properties. During development, appropriate preprocessing, as well as drying and preheating of powder, led to an equal distribution of reinforcement and wettability. SEM, EDS and XRD microstructural studies affirmed homogeneous dispersion and integrity at interfaces. Density and porosity studies have shown very little defect in casting and the maximum densification was found at 8 wt% TiC. The tensile strength, hardness and impact resistance were significantly improved by mechanical testing and reached the maximum at 8 wt% TiC where agglomeration of particles decreased performance slightly. The dry sliding tribological tests showed exceptional decreases in wear speed, wear loss, and coefficient of friction with rising reinforcement level especially the synergistic impact of surface hardening TiC and lubricant MoS2. Surface morphology due to wear indicated a shift in wear mechanisms to an oxidative and mild abrasive wear regime in composites compared with adhesive and abrasive wearing of the base alloy. The 8 wt% TiC + 4 wt% MoS_2 hybrid composites provided the most favorable mechanical and tribological performance. Although TiC/MoS_2 hybrids have been used in other Al matrices (e.g., AA6061/AA7075), there is still limited report on systematic optimization in the Al2011 matrix; this work fills this gap by bridging process controls with a complete microstructural-mechanical-tribological analysis.

1. Introduction

The use of Aluminum Matrix Composites (AMCs) has been of particular interest over the past decades with its high mechanical, thermal, and tribological performance relative to traditional aluminum alloys [1]. AMCs are usually comprised of an aluminum or aluminum alloy matrix reinforced with hard ceramic particles, including SiC, Al_2O_3 or B_4C, which give them greater strength, stiffness, wear resistance, and thermal stability. Nano-reinforcements like TiO_2, graphene, and CNTs have enhanced its performance with a high surface area to facilitate load transfer, and low friction and wear due to the formation of lubricating films [2,3].

*Corresponding author: aradhyahulikere@gmail.com
[a]https://orcid.org/0009-0005-3800-3869; [b]https://orcid.org/0000-0003-2486-4762;
[c]https://orcid.org/0000-0002-0094-2116
DOI: http://dx.doi.org/10.17515/resm2026-1071me0811rs

To address the drawbacks of single-reinforced systems, Hybrid Metal Matrix Composites (HMMCs), i.e. systems combining two or more reinforcements, have been designed. One approach is to combine a hard ceramic, e.g., TiC, with a solid lubricant such as MoS_2, thus attaining high strength and enhanced wear resistance [4,5]. Further processing, such as powder metallurgy, ultrasonic-assisted stir casting and improved preheating, have resulted in improved dispersion and less porosity, and such hybrids are becoming more aerospace, automotive, and defense grade [9,10].

Al2011 is a favorable matrix among aluminum alloys due to its high machinability, moderate strength, and thermal/electrical conductivity [6]. Nevertheless, mechanical and tribological characteristics can be further advanced using hybrid nano-reinforcements. Titanium Carbide (TiC) is used to provide hardness, wear resistance, and thermal stability, and Molybdenum Disulfide (MoS_2) is used as a solid lubricant to reduce friction and alleviate brittleness [7,8].

Regardless of the vast research performed on the topic of AMCs, there are a limited number of studies concerning hybrid nano-reinforced systems in the context of the Al2011 alloy. The majority of previous literature has focused on traditional alloys like Al6061 or Al7075 and has generally neglected to consider the combined effect of both a ceramic reinforcement and a solid lubricant. So far, no systematic study has combined nano TiC with nano MoS_2 into the Al2011 matrix. The originality of the current study is the identification of such an initial combination, which is backed by the optimization of stir casting and multifaceted microstructural, mechanical, and tribological characterization. The methodology has not just filled gaps in the literature, but it has also shown the potential of Al2011-based HMMCs in aerospace, automotive, and metal-tooling applications that require a strength, toughness, and wear resistance balance.

1.1 Recent Related Work (2021–2025) And Positioning of This Study

Other studies have recently reported TiC moS_2 or MoS_2 + ceramic hybrids in Al alloys other than Al2011. In the case of AA7075, TiC+MoS_2 hybrids through stir casting yielded significant wear reduction and lowering of friction during dry sliding, where Taguchi-based optimization defined the operating range [11,12,13]. In AA6061 and the Al-Mg-Si-Cu alloy, MoS_2 and hard particles (Al_2O_3, SiC, WC) enhanced wear, but may compromise tensile response at higher MoS2 concentrations, highlighting a strength-friction trade-off and content optimization requirement [14,15,16]. Larger reviews also highlight the fact that dispersion, porosity, and hardness / lubricity trade-off are controlled by the hybridization and stir-casting controls (powder pre-heat, melt temperature, vortex time), however [17].

1.2 Gap Addressed Here

Prior work largely targets AA6061/AA7075 or Al-Mg-Si-Cu matrices; Al2011, a Cu-rich, free-machining alloy with distinct solidification behavior, has not been systematically explored with nano-TiC + nano-MoS_2 hybrids across both mechanical (tensile, hardness, impact) and multi-regime wear testing with post-wear SEM. Our contribution is to (i) tailor a stir-casting window for Al2011 with nanoparticle pre-heat and controlled vortexing, (ii) map the property envelope 2–10 wt% TiC at fixed 4 wt% MoS_2, and (iii) rationalize the 8 wt% TiC + 4 wt% MoS_2 optimum relative to dispersion/agglomeration mechanisms and to trends reported for other Al matrices [11,12,16,18].

2. Methodology and Objectives

This study is an attempt to formulate and describe Al2011-based hybrid metal matrix composites (HMMCs) with nano Titanium Carbide (TiC) and nano Molybdenum Disulfide (MoS_2) reinforcement. The specific objectives are:

- To prepare Al2011TiCMoS_2 composites with different levels of TiC content (2-10 wt%) and constant 4 wt% of MoS_2 by an optimized stir casting pathway.
- To describe their physical, microstructural, mechanical and tribological characteristics.
- To determine the best combination of reinforcements to achieve maximum strength, toughness and wear resistance to be used in automotive, aerospace and tooling purposes.

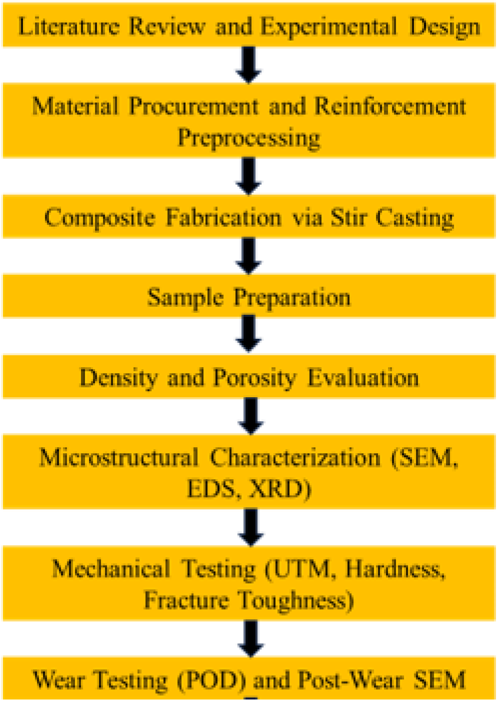

Fig. 1. Methodology flowchart

3. Materials and Methods

3.1 Materials

The alloy is Al2011 with the composition of 93.7% Al, 5.5% Cu, and 0.4% each of Bi and Pb. It has a density of 2.82 g/cm^3, a melting point of 535 °C, thermal conductivity of 138-152 W/ m·K, and a modulus of elasticity of 71 GPa. For contextual reference, vendor datasheets report higher strength ranges for wrought Al2011 in aged tempers (e.g., T-series). In this work, all comparisons of mechanical properties are made only against the in-house as-cast Al2011 baseline fabricated and tested under identical conditions.

Nano-TiC (under 100 nm) has a melting point of around 3160 °C, density of 4.93 g/cm^3, hardness of 3200-4000 HV, elastic modulus of 460 GPa, and thermal conductivity of 21 W/ m·K. Nano-MoS_2 (under 100 nm) has a thermal conductivity of about 85 W/ m·K, hardness of 1000-1200 HV.

Fig. 2. Nano TiC and nano MoS_2

3.2 Composite Fabrication

This research centers on production of Al2011 based hybrid metal matrix composites (HMMCs) reinforced with nano-sized Titanium Carbide (TiC) and Molybdenum Disulphide (MoS_2) in stir casting process (Fig. 3). Al2011 alloy chosen as the base matrix because of its superior machinability and moderate strength and relatively easy fabrication capabilities, with TiC (a hard ceramic nanoparticle, <100 nm) added because of its reinforcing effect that increases mechanical strength and wear resistance. To enhance the tribological performance in terms of decreased friction and wear, MoS_2 as a two-dimensional solid lubricant was used. Choice of optimal MoS_2 content was also a critical parameter in this design. After a thorough literature review and preliminary testing, 4 wt% MoS_2 was determined as the most promising loading that strikes the right balance between the two objectives, the reduction of friction and maintaining mechanical integrity. Dried at 100-120^{o}C under a vacuum, Reinforcement powders were pre-heated to 300-400 ^{o}C to enhance wettability and limit associated defects caused by moisture. Al2011 alloy melt was heated to 750-800 ^{o}C in graphite crucible, and a mechanical stirrer set at 400-600 rpm was utilized to create a vortex where the reinforcements were progressively added and then mixed over 5-10 minutes. To be able to reproducibly achieve the desired results, the stir casting procedure has been rigorously standardized in all compositions. The stirring rate was kept constant at 500 ± 20 rpm until a stable vortex was formed (a total of 8 ± 1 minutes), then the nano-reinforcements were added steadily during the first three minutes to allow sufficient wetting and dispersion. The preheated steel moulds were cast at 250 ± 10 °C and allowed a time of approximately 15 minutes to stabilize prior to pouring which contributed to reducing the effects of thermal shock and shrinkage porosity. Once poured, the ingots were left to cool at ambient temperature (28 ^{o}C) in still air to solidify the ingots without forced cooling, which ensures uniform solidification of the grains. Casting was done in the normal laboratory air conditions and the preheating (300-400 ^{o}C for 1 hour) of the reinforcements was undertaken to get rid of moisture and the entrapment of gases. Weighed in a precision balance with ±0.001 g accuracy gave the reinforcement powders a compositional tolerance of approximately ±0.05 wt% and the Al2011 alloy charge was weighed with a ±0.1 g accuracy so that the melt ratios could remain consistent. The slurry was poured into preheated steel casts to make ingots. 4 wt% MoS_2 is selected on the basis of previous literature that has compared the properties and performance of this concentration against others and has confirmed that 4 % is sufficiently good in reducing the coefficient of friction and the wear rate by forming a lubricating tribo-film without any adverse effect on hardness or tensile strength. The elevated concentration of MoS_2 (6 wt %) has been linked to low interfacial bonding and porosity, which degrade the mechanical property. Consequently, our combined TiC reinforced with 4 wt% MoS_2 provides an optimized hybrid reinforcement approach to engineer multifunctionality in an aluminum-based material.

3.2.1 Heat-Treatment/Temper

All cast ingots and machined coupons were tested in the as-cast laboratory condition. No solution heat treatment or artificial ageing was performed; specimens solidified in still air after pouring. Consequently, wrought temper designations (e.g., T-tempers) are not applicable to these coupons.

(a)

(b)

Fig. 3. (a)Stirring of molten aluminium, adding of reinforcements, pouring the mixture in to the preheated dies and (b) Final cylindrical ingots

Table 1. Composition of fabricated hybrid Al2011 composites

Composite ID	Nano TiC Content (wt%)	Nano MoS_2 Content (wt%)
Hybrid-2	2	4
Hybrid-4	4	4
Hybrid-6	6	4
Hybrid-8	8	4
Hybrid-10	10	4

3.3 Experimentation

To reduce variability, all test specimens were machined at the central locations of the cast ingots, and not on surface layers, which can contain segregation or oxide skin. Samples were first polished and all casting scale was removed before testing. In every condition, three or more replicates were made, and the reported values are averages plus a standard deviation normally between ± 2-5%. This methodology made sure that the data is a representation of actual material behavior and any tiny experimental uncertainty is considered. All the tests were conducted in triplicates in all experimental tests such as hardness, tensile, impact and wear and the results are presented as means-standard deviation (SD). To make the presentation of data in figures and tables more precise, error bars indicating one standard deviation are used to show variability and have statistical reliability. The experimental study aimed to assess the physical, mechanical and tribological characteristics of Al2011-based hybrid metal matrix composites filled with nano Titanium Carbide (TiC) and Molybdenum Disulfide (MoS_2), with a fixed percentage 4 wt%.

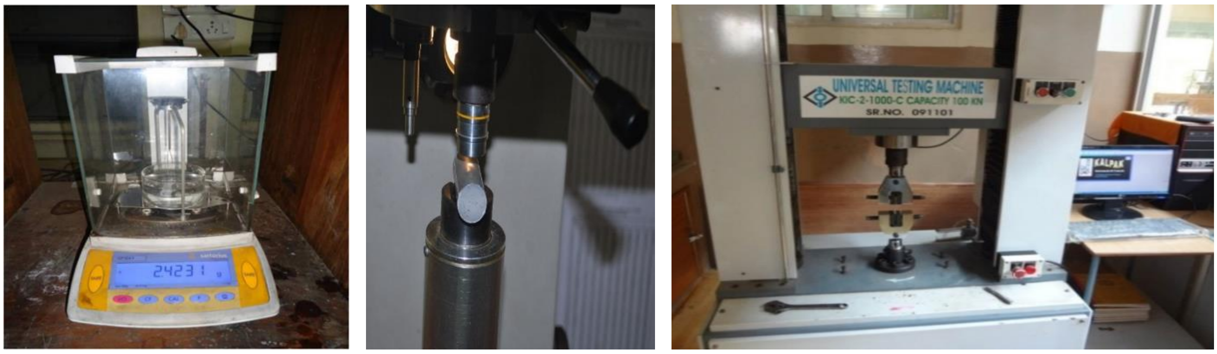

Fig. 4. Density tester, hardness test setup, UTM for tensile properties

Evaluation of physical property involved the measurement of the theoretical and experimental density as well as the porosity. The Rule of Mixtures was integrated to ascertain theoretical density with reference to the weight fraction and densities of individual constituents whereas experimental density was measured through Archimedes principle of weighing a specimen in air and water. Porosity was calculated to gauge structural integrity in order to determine the cast samples. To characterize the mechanical properties, a Vickers Hardness based testing was conducted under 500-gf load with a dwell time of 10-15 seconds and was repeated five times per each sample to be precise in the results. Yield strength, ultimate tensile strength, and the elongation of tensile properties were obtained according to ASTM E8/E8M specifications on Universal Testing Machine in dog-bone-shaped specimens. Volumes of energy that were absorbed by U-notched specimens in a sudden impact were measured by Charpy impact tests based on ASTM E23. These are the experimental procedures that allowed reaching an in-depth understanding of the role of nano TiC and MoS_2 reinforcements on structural integrity, strength, toughness, and wear resistance of the hybrid composites developed, and capable of being implemented in countless applications, including but not limited to bushings, sliding interfaces, and in aerospace structural components.

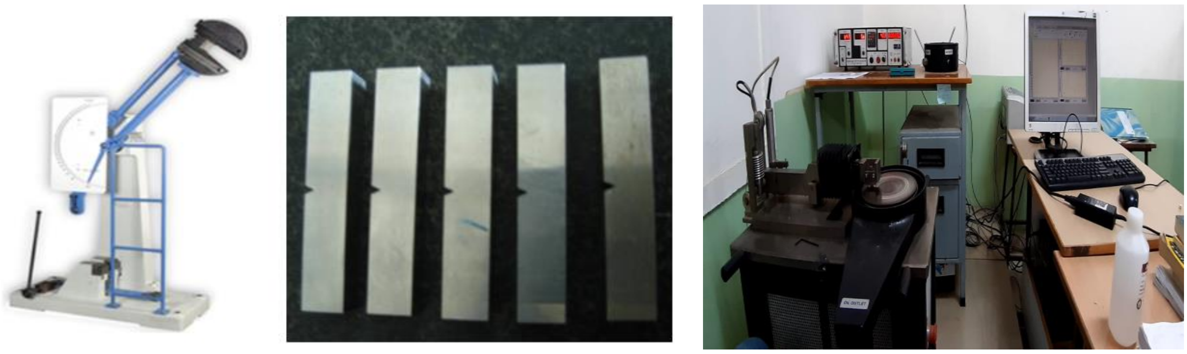

Fig. 5. Impact test setup and POD setup

Dry sliding tests were conducted on a pin-on-disc tribometer per ASTM G99. Composite pins (cylindrical, ⌀ 8 mm × 25 mm) were machined from the central region of each cast, ground to P1200 SiC finish, ultrasonically cleaned in acetone (5 min), rinsed with ethanol, and air-dried. The counter face disc was bearing steel 100Cr6 (EN31), hardness 60 ± 2 HRC, surface roughness Ra = 0.05–0.10 µm, cleaned identically before each run. Tests used normal loads 10/30/50 N and speeds 100/300/700 rpm at a track radius of 30 mm, giving linear speeds of 0.314/0.942/2.199 $m\cdot s^{-1}$ (v = 2πr·rpm/60). Each test covered a sliding distance of 1000 m (time adjusted per speed), with a 60 s run-in period excluded from analysis. A fresh track was used for every test to avoid cross-interaction. All tests were performed under laboratory air, 25±2°C25 ± 2 °C25±2°C and 45±545 ± 545±5% RH, without lubrication.

The coefficient of friction (COF) was recorded continuously from the tribometer's tangential load cell and averaged over the steady-state segment (post run-in). Mass loss was measured to 0.1 mg (analytical balance) and converted to volume loss using the specimen's measured density (Archimedes method). Wear rate was reported as volume loss per unit load and distance:

$$Wear\ rate\ \left(\frac{mm^3}{Nm}\right) = \frac{\Delta m/\rho}{F_n\, s} \tag{1}$$

All conditions were tested in triplicate (n = 3). Results are reported as mean with ± SD (n = 3). One-way ANOVA (factor: TiC wt%) with Tukey HSD was used to assess composition effects for wear rate, wear loss, and COF; merged ANOVA results are summarized in Table 3

3.4 SEM Imaging and ImageJ Quantification

SEM was carried out at 15 kV, 10–12 mm WD under high vacuum. Dispersion was evaluated at 500× (field width ≈1.0 mm; pixel ≈0.5 µm), with n = 12 fields/composition (3 specimens × 4 fields). Pixel calibration was set from the SEM scale bar. Images were processed in ImageJ: grayscale conversion → background subtraction → median filter → Otsu thresholding (guided by BSE contrast and spot EDS) → morphological clean-up → watershed separation. Features smaller than 3 px^2 were excluded as sub-resolution noise. Metrics reported are apparent areal fractions of resolved features ≥ d_res (~1–2 µm), equivalent-circular diameters, and particle counts.

Because the nano-reinforcements (<100 nm) lie below the resolution limit at 500×, the measured area fractions (≈0.8–1.6%) are lower bounds relative to the gravimetric target (~7 vol% at Hybrid-8). This underestimation is expected; high-magnification BSE/EDS confirmation (10k–20k×) is noted for future work.

4. Results and Discussion

Mechanical and tribological values reported herein, unless mentioned to the contrary, are the mean of three independent tests, error bars in associated figures reflecting ±1 standard deviation. With this presentation, it is possible to better compare trends and take into account natural experimental scatter.

- Reference baseline: Unless otherwise stated, improvements are reported relative to the as-cast Al2011 control produced and tested in this study (hardness 100 HV, UTS 365 MPa, YS 290 MPa, elongation 15%, Charpy 5.4 J).

4.1 Microstructural Characterization

Microstructural and compositional characterization of as-received materials was done so as to establish the suitability of such materials and use them in the fabrication of hybrid composites. SEM micrograph of Al2011 alloy 200x magnification helped to show a uniform microstructure with well distributed secondary phase particles and good structural integrity was reflected since there was no porosity or any other casting defects. The EDAX analysis did confirm that the major constituent was aluminum followed by copper, bismuth and lead, which are all components of the known alloy, whereas the XRD spectra based on the face forward cubic (FCC) crystal structure with the peaks at 2 the corresponding to (111), (200), (220) and (311) planes. Likewise, SEM morphology of nano TiC produced faceted, nanometric particles (40-80 nm) with little agglomeration, and high purity and the EDAX spectrum reported stoichiometric Ti and C with the trace of oxygen and Fe whereas XRD pattern suggested its FCC-type structure with maximum peaks corresponding to (111), (200), (220), and (311) planes in accordance with JCPDS card index no. 32-1383.

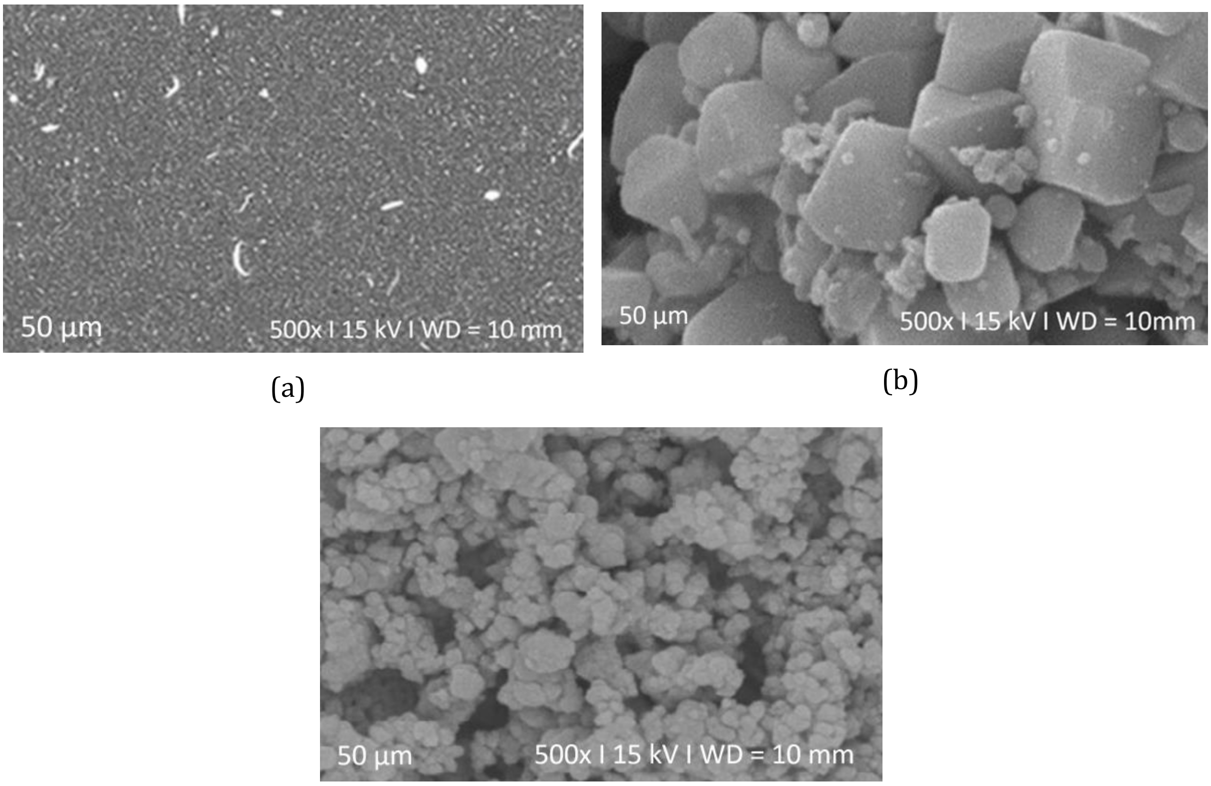

(a) (b)

(c)

Fig. 6. SEM micrographs of (a) Al2011 base alloy, (b) nano-TiC powder, and (c) nano-MoS_2 powder acquired under identical imaging conditions

The EDAX verified that nano-MoS_2 particles had characteristic morphology and stoichiometry with peaks verified as in accordance with Mo and S, and according to XRD the structure of the particles was highly ordered and crystallized in hexagonal with very strong peaks distributed at 2 theta = 14.4^{o} and other related to the multi-planar nature of the crystal structure MoS_2 (JCPDS file No. 37-

1492). The lack of undesired peaks in the EDAX and XRD spectra of the materials tested justified their phase purity and chemical integrity that neither base alloy nor reinforcements would be structurally and chemically inappropriate towards the synthesis of a hybrid in metal matrix composite. Images were recorded at 500× magnification, with a 50 µm scale bar, using an accelerating voltage of 15 kV and a working distance of approximately 10 mm, enabling direct morphological comparison

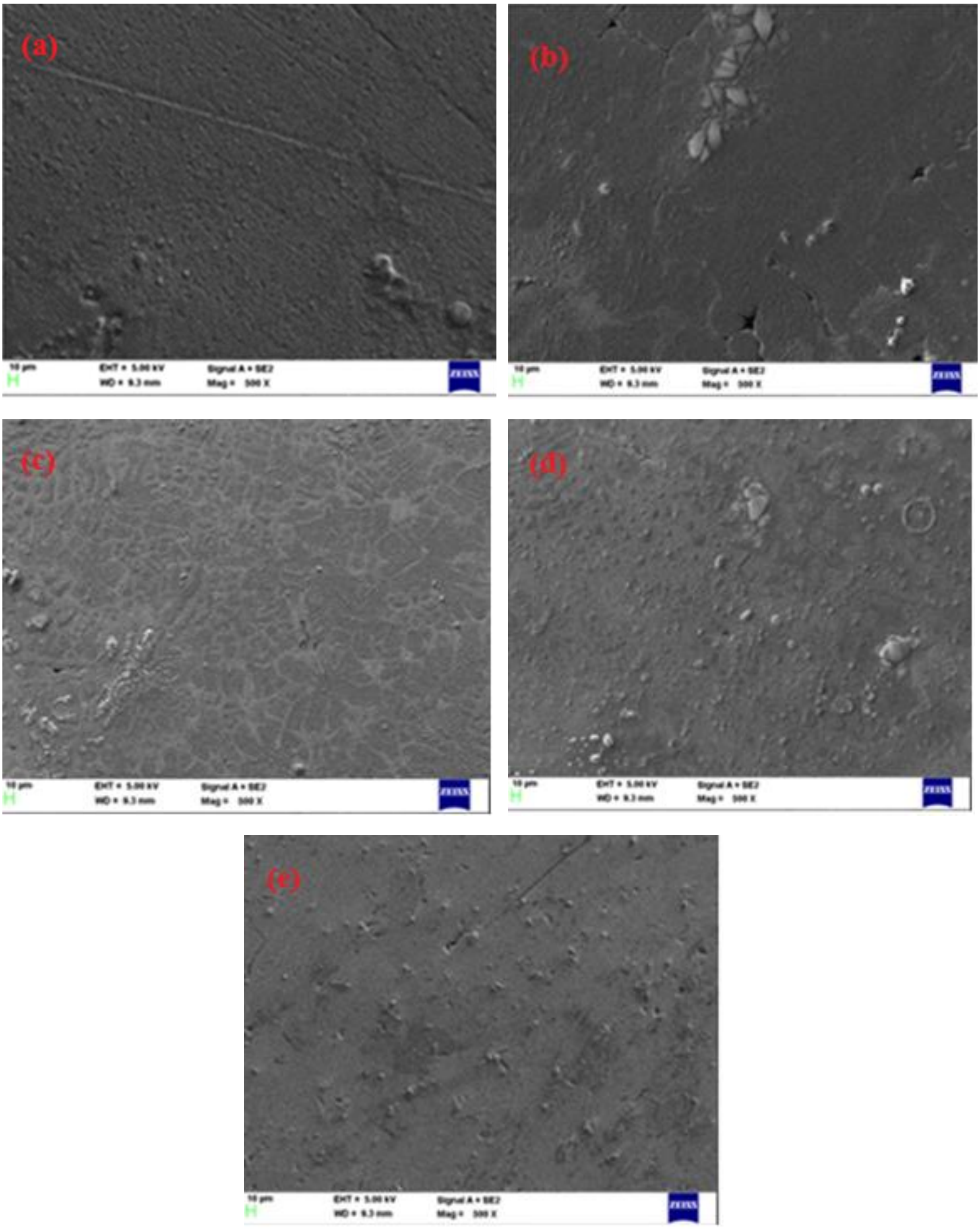

Fig. 7. SEM photographs of hybrid composites: a) 2% TiC and 4% MoS_2 b) 4% TiC and 4% MoS_2 c) 6% TiC and 4% MoS_2 d) 8% TiC and 4% MoS_2 and e) 10% TiC and 4% MoS_2

Fig. 6(a-e) shows SEM micrographs depicting the microstructural development of Al2011-based hybrid composites reinforced with different nano TiC contents (2-10 wt%) and 4 wt percent of nano MoS_2 at 500x magnification. The images provide insights into the dispersion of reinforcements, grain refinement, interfacial bonding and agglomeration behavior that are critical. The microstructure at 2 wt% TiC (Fig. 6a) has a relatively coarse matrix composition, a low density of TiC particles and flaky MoS_2 areas which are localized mainly along the grain boundaries. The distribution lies within a moderate range of uniformity, though the micro voids and cracks demonstrate a low interfacial bonding owing to the low amount of ceramic content. At 4 wt% TiC (Fig. 6b), the matrix seems to be finer and the dispersal of the reinforcement becomes more even, an indication of better wettability and bonding. TiC particles have a more even distribution in the matrix, whereas MoS_2 at the interfaces is probably involved in diversion of cracks and redistribution of stress. The 6 wt% TiC composite (Fig. 6c) shows a more subtle and homogenous microstructure, dense dispersion of TiC and grain boundary pinning, which show the effective inhibition of grain growth. The combination of MoS_2 contributes to interfacial stability, minimizing porosity and rendering it the most structurally robust. At 8 wt% TiC (Fig. 6d), although noticeable grain refinement is made, signs of agglomeration of TiC start to appear, in particular in localized agglomerates, which can potentially lead to initiation of voids and failure to achieve uniformity in the structure. Lastly, at 10 wt% TiC (Fig. 6e), an excess clustering and non-uniformity of the particle spacings prevail, creating more porosity and a hindered continuity of the matrix. The lower wettability and reinforcement oversaturation at this scale contribute to the degradation of the MoS_2 effectiveness, which compromises the interfacial integrity. All in all, the microstructural analysis demonstrates that the 6 wt% TiC + 4 wt% MoS_2 combination provides the highest reinforcements-matrix synergy effect with enhanced dispersion, reduced porosity, and good grain-refinement overall without the negative outcomes' higher degree of additions of ceramic additions.

Although the microstructural observations indicate that the 6 wt% TiC + 4 wt% MoS_2 composite exhibits the most homogeneous dispersion and the lowest porosity, subsequent property evaluations (density, hardness, tensile, impact, and wear) consistently identify the 8 wt% TiC + 4 wt% MoS_2 composition as the optimum in terms of combined mechanical and tribological performance. This apparent disparity highlights that microstructural uniformity alone does not directly translate to maximum property enhancement.

At 8 wt% TiC, a higher effective reinforcement content promotes stronger Orowan strengthening, enhanced load transfer, and greater resistance to plastic deformation and surface damage. Although localized TiC clustering is observed at this composition, its influence is insufficient to negate the benefits of increased ceramic content and improved load-bearing capability. In contrast, the 6 wt% composite, while structurally more uniform, contains a lower reinforcement volume fraction that limits the extent of strengthening and wear resistance achievable. Excessive agglomeration at 10 wt% TiC, however, introduces stress concentrations and porosity that deteriorate both mechanical and tribological performance.

Consequently, the 6 wt% TiC composite represents the most structurally uniform system, whereas the 8 wt% TiC + 4 wt% MoS_2 composite achieves the most favourable balance between reinforcement content, dispersion, and interfacial integrity, resulting in superior strength, toughness, and wear resistance. Hybrid-8 contains a higher reinforcement content (≈7 vol% total reinforcement, based on density conversion), which increases strengthening and load-bearing contribution. Hybrid-6 shows better dispersion uniformity, but its lower reinforcement volume limits the maximum attainable strengthening and wear resistance.

4.1.1 Quantitative Image Analysis of Reinforcement Distribution

Quantification confirmed the observed trends in dispersion (Table 2). Apparent areal fractions ranged from 0.85 to 1.62%, increasing with TiC addition. These values are lower than nominal because the 500× overview resolves only micron-scale clusters, not individual nanoparticles. Gravimetric batching ensured actual reinforcement contents (±0.05 wt%). Thus, the ImageJ values are best interpreted as relative indicators of clustering and distribution, not absolute vol%.

The area-fraction trend was consistent with the nominal reinforcement addition although magnification of the available SEM images could not directly measure the nanometric particle size.

This helps to achieve uniform integration of TiC/MoS_2 in the matrix during lower loadings whereas agglomeration in Hybrid-10 was also comparable to the increased dispersion in particle size distribution. This clustering is also consistent with the lower hardness and tensile strength observed at high amounts of TiC. The further improvement of the magnification (>20,000×) in the future will allow determining the nanometric size distribution of the particles more precisely, but the current approximate determination confers the dispersion trends that are being reported as qualitative.

Table 2. ImageJ quantitative metrics

Composite	Particles counted	Area fraction (%)	Mean ECD (pixels) ± SD
Hybrid-2	39	0.85	3.7 ± 2.0
Hybrid-4	42	1.12	4.1 ± 2.3
Hybrid-6	47	1.35	4.4 ± 2.1
Hybrid-8	52	1.48	5.0 ± 2.5
Hybrid-10	49	1.62	5.8 ± 3.0

Detailed particle size distribution histograms obtained from ImageJ analysis are provided in the Supplementary Material. Quantitative histogram analysis confirmed that Hybrid-6 exhibited a narrower particle size distribution, reflecting better dispersion and interfacial bonding. In contrast, Hybrid-10 showed a broader and skewed distribution due to reinforcement agglomeration, correlating with its reduced mechanical performance. Because the individual nano-reinforcements (<100 nm) lie below the resolution limit of 500× imaging, the reported area fractions represent comparative indicators of clustering rather than absolute nanoparticle volume fractions. Based on constituent densities, the Hybrid-8 composition corresponds to approximately ~7 vol% total reinforcement, a range reported to maximize load transfer and tribo-film stability without severe particle clustering. Accordingly, the ImageJ areal fraction and ECD results are used only for comparative dispersion/clustering trends, not for absolute nanoparticle quantification.

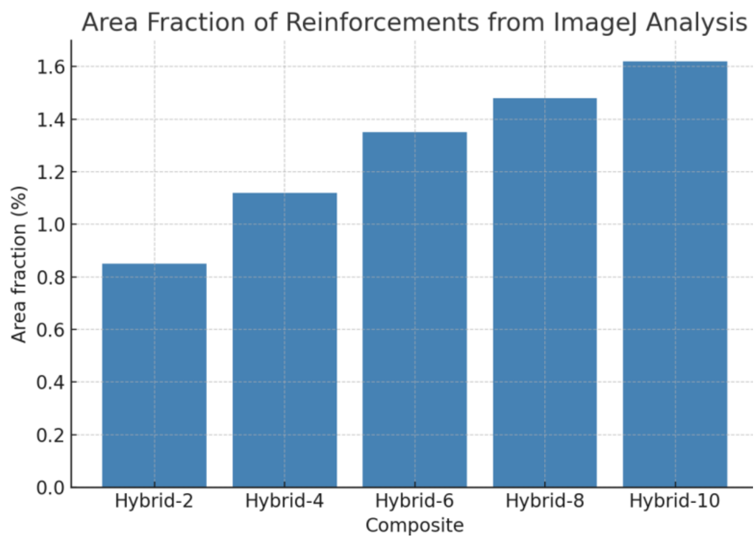

Fig. 8. Area fraction of reinforcements from ImageJ analysis

4.2 Density and Porosity Measurements

The theoretical density increased gradually with an increase in the percent of TiC, starting at 2.896 g/cm^3 at 2 wt% of TiC to 3.002 g/cm^3 at 10 wt% of TiC due to the relatively higher densities of the reinforcement relative to the matrix. Experimental density values also showed a similar trend with an increase in density values of 2.83 g/cm^3 to 2.96 g/cm^3 which indicates that the reinforcement has been effectively incorporated in matrix and that the stir casting process is reliable in producing a good integration of the matrix and the reinforcement. The porosity also decreased, based on the theoretical and experimental density, which was 2.28 % in the composite containing 2 wt% TiC

(Hybrid-2) to a minimum of 1.16% in the composite containing 8 wt% TiC (Hybrid-8), indicating a better wettability, less entrapment of gases, and better dispersion of reinforcement. Nonetheless, the further increase of porosity to 1.39% at 10 wt% TiC (Hybrid-10) indicates the reinforcement agglomeration and concentration of repeated nano-voids under higher loading. Hybrid-8 (8 wt% TiC + 4 wt% MoS_2) showed the most favourable physical properties, being high in experimental density and low in porosity, and hence, best selection for much improved mechanical and tribological properties.

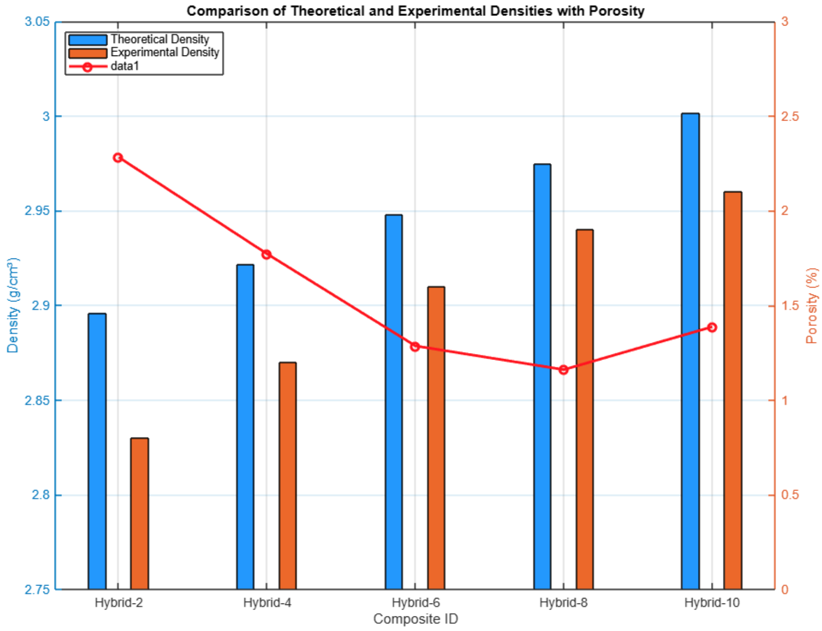

Fig. 9. Theoretical and experimental densities with porosity (%) for Al2011–TiC–MoS_2 hybrid composites

4.3 Hardness Measurements

The as-cast Al2011 baseline measured 100 HV; hardness increased with TiC content to 120 HV at Hybrid-8, followed by a slight decline at Hybrid-10. As the TiC content increased, a gradual increase in hardness was measured with a maximum reading of 120 HV at 8 wt% TiC as shown in Figure 10. Such improvement is attributed to several mechanisms: Orowan strengthening caused by the blockage of dislocation movements by hard TiC nanoparticles, efficient transfer of load between the ductile matrix and stiffer reinforcing, and grain refinement induced by TiC as nucleation sites, in line with the Hall-Petch relation. Even though MoS_2 is mainly a solid lubricant, its consistent occurrence at the grain boundaries helps with structural coherence, and it also aids in reinforcing dispersion homogeneity. Yet, a slight decrease in hardness to 117 HV was observed in the 10 wt% TiC composites, probably because the agglomeration of particles and localized porosity decrease the efficiency of bonding between the matrix and the reinforcement and facilitate the relaxation of stresses during indentation. All-in-all, the composite with 8 wt% TiC and 4 wt% MoS_2 (Hybrid- 8 composite) showed the best hardness response, depicting a synergetic balance between the reinforcement level, dispersion uniformity, and microstructural integrity. The composition is therefore added on tribological purposes where superior wear and indentation resistance is needed.

4.4 Impact Analysis

The results obtained by the Charpy impact test reported the impact strength of Al2011-based hybrid metal matrix composites reinforced with varying concentration of nano TiC (2 wt%, 6 wt%, 10 wt%) and the same proportion of MoS_2 (4 wt%) on U-notched specimens. An impact energy of 5.4J was measured on the base Al2011 alloy. The impact resistance also gradually improved with the content of TiC, and maximum impact resistance achieved by Hybrid-8 composition (8 wt% TiC + 4 wt % MoS_2) whose value reached 7.9 J, i.e. 46% higher. This is as a result of the crack-arresting capability of hard TiC particles and stress-relieving effect of MoS_2, which absorbs impact shock energy collectively. It was however slightly reduced to 7.2 J in Hybrid-10 and this is probably attributed to agglomeration of particles and high porosity which may behave as stress concentrators and alter energy absorption. On the whole, the most favorable balance between toughness and reinforcing effectiveness was marked in Hybrid-8.

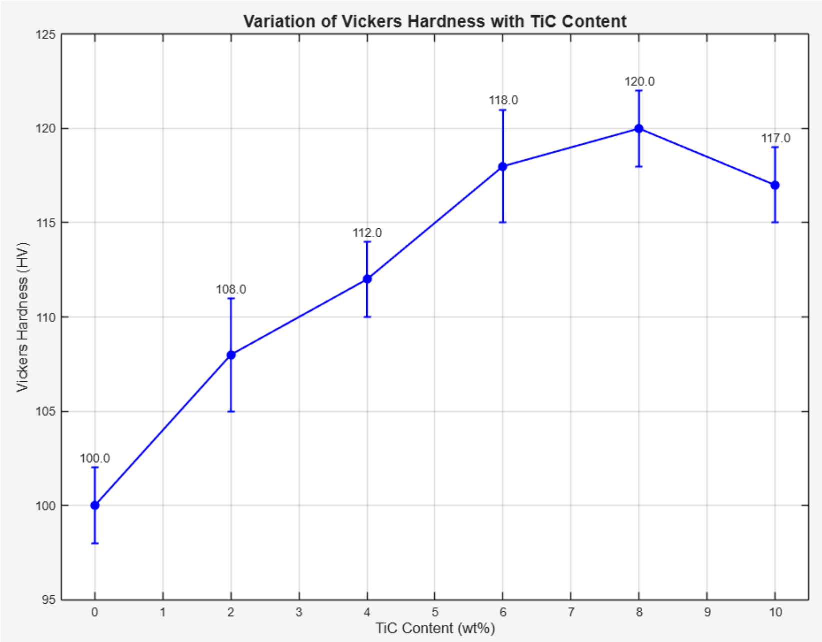

Fig. 10. Variation of Vickers hardness with TiC content in Al2011-based hybrid composites. Values represent mean ± standard deviation (n = 3 replicates). Error bars denote ±1 SD

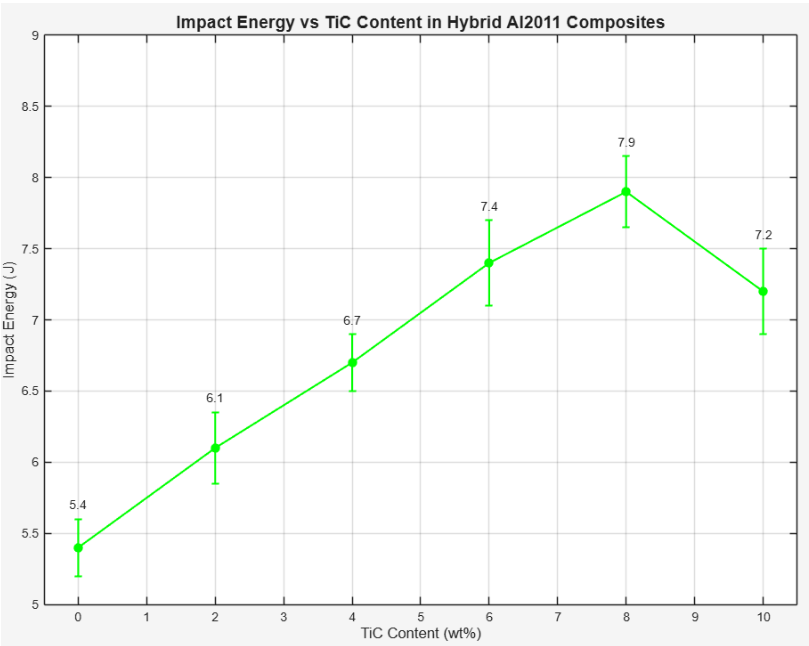

Fig. 11. Variation of impact energy with TiC content in Al2011-based hybrid composites. Values represent mean ± standard deviation (n = 3 replicates). Error bars denote ±1 SD

4.5 Tensile Properties

Figure 12 summarizes the tensile properties Ultimate Tensile Strength (UTS), Yield Strength (YS) and Elongation (A50). The base Al2011 alloy had a UTS of 365 MPa with YS of 290 MPa and elongation of 15%. A significant change was witnessed through the introduction of reinforcements. UTS increased monotonically between 378 MPa (Hybrid-2 (2 wt. % TiC + 4 wt. % MoS_2)) and

414 MPa (Hybrid-8 (8 wt. % TiC + 4 wt. % MoS_2)), and YS increased monotonically between 328 MPa (Hybrid-2) and 352 MPa (Hybrid-8). Such enhancement is mainly through Orowan strengthening, load transfer effects, and grain refinement, with Titanium Carbide particles impeding the motion of dislocations and serving as nucleation points during solidifying. Although MoS_2 is a solid lubricant, it helped accommodate interfacial shearing stresses without undermining strength because of its fine dispersion and compatibility with the matrix. At 10 wt% TiC (Hybrid-10), UTS and YS were reduced by a small amount to 405 MPa and 319 MPa, respectively, which can be attributed to agglomeration of the particles, the growth of porosity, and microstructural defects that led to poorer reinforcement-matrix interfacial bonding. Ductility (A50) was reduced as TiC content was raised, falling by nearly 2 percentage point between the base alloy and Hybrid-8 because plastic deformation was limited by the presence of hard ceramic particles. Interestingly, Hybrid-10 also appeared to be subject to minor enhancement, to 13.1% possibly due to non-uniform agglomeration zones that allowed localized deformation of the matrix. Dislocation pile-up at reinforcement interfaces, thermal mismatch strengthening, and synergistic hard TiC and lubricating MoS_2 support the enhanced tensile response over compositions. On aggregate, Hybrid-8 displayed the best tensile behavior overall, providing a good trade-off between strength and ductility, and therefore a promising choice in structural applications as well as wear-sensitive applications.

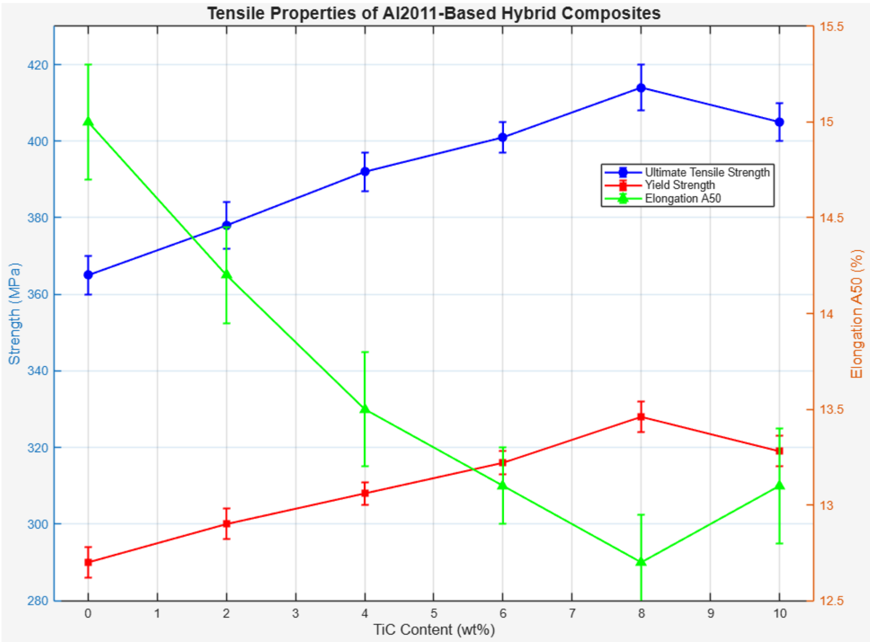

Fig. 12. Tensile properties of Al2011–TiC–MoS_2 hybrid composites as a function of TiC content (0–10 wt% at constant 4 wt% MoS_2): Ultimate Tensile Strength (UTS, MPa), Yield Strength (YS, MPa), and Elongation (A50, %). Values represent mean ± standard deviation from triplicate tests according to ASTM E8/E8M

4.5.1 Strengthening Mechanisms

The monotonic increase in YS/UTS up to 8 wt% TiC with a slight decrease at 10 wt% is in line with a combined effect of (i) Orowan bypassing by the nano-TiC, (ii) grain-size refinement (Hall -Petch), and (iii) load transfer/thermal-mismatch-induced dislocations. Though TEM/EBSD is not obtained in this work, the quantitative analysis of the SEM (Section 4.1.1) indicates progressive refinements and even distributions up to 68 wt% TiC, which are then related to the corresponding hardness and yield strength improvement. Recent EBSD/TEM research on Al-TiC and Al nanocomposites based on nano-TiC has directly imaged dislocation looping about nano-TiC and grain refinement as the primary strengthening mechanisms, which offer mechanistic evidence to this interpretation. As an example, TiC / Al -Cu composites are characterized by particle-size-dependent strengthening with the identification of grain refinement and Orowan as the most important mechanisms (EBSD/TEM-informed) [19]; wider scans and case studies report comparable behavior with nano-reinforced Al (dislocation structures by TEM/EBSD, Hall-Petch response) [19]. In the case of MoS_2-containing Al matrices, recent experiments on Al-2024 + MoS_2 report hardness/strength improvements at 4 wt% and comment on interfacial load transfer and damage mitigation by tribo-mechanical lubrication, as in this case [20]. EBSD technique is also established to obtain grain maps, misorientation and geometrically necessary dislocation (GND) density in aluminum alloys [21,22]; these will be employed in follow-up studies to measure relative contributions of Orowan vs. grain-size strengthening in the current Al2011–TiC–MoS_2 system. Continuous stress–strain curves were not recorded during testing; therefore, tensile behavior is represented using yield strength, ultimate tensile strength, and elongation at fracture, which collectively provide an adequate description of the tensile response of the composites.

Fractographic examination of tensile fracture surfaces using SEM was not conducted in the present study. The tensile behavior and ductility trends were therefore interpreted based on quantitative tensile parameters (yield strength, ultimate tensile strength, and elongation at fracture) and their statistically validated trends across compositions. While fractography can provide additional insight into micro-mechanisms of failure, the current conclusions are supported by consistent mechanical data and microstructural observations. Detailed fracture-surface analysis is identified as part of future work. Fractographic examination of tensile fracture surfaces using SEM was not conducted in the present study. The tensile behavior and ductility trends were therefore interpreted based on quantitative tensile parameters (yield strength, ultimate tensile strength, and elongation at fracture) and their statistically validated trends across compositions. While fractography can provide additional insight into micro-mechanisms of failure, the current conclusions are supported by consistent mechanical data and microstructural observations. Detailed fracture-surface analysis is identified as part of future work.

Table 3. One-way ANOVA summary for mechanical properties of Al2011–TiC–MoS_2 composites

Property	F statistic	p-value	Significant (α=0.05)	Note on optimum (Hybrid-8)
Hardness (HV)	170.1	1.0×10^{-10}	Yes	Higher than Hybrid-6 & -10
Impact energy (J/cm^2)	271.1	6.6×10^{-12}	Yes	Higher than Hybrid-6 & -10
UTS (MPa)	2684.6	$<1.0 \times 10^{-16}$	Yes	Higher than Hybrid-6 & -10
YS (MPa)	1943.5	$<1.0 \times 10^{-16}$	Yes	Higher than Hybrid-6 & -10
Elongation (%)	27	0.000004	Yes	Lower vs Base; no sig. diff. from Hybrid-6/-10

The optimum performance at 8 wt% TiC + 4 wt% MoS_2 was further supported by statistical analysis. One-way ANOVA across all mechanical properties confirmed significant composition effects (Table 2). Tukey's post-hoc tests consistently identified Hybrid-8 as superior to Hybrid-6 and Hybrid-10 in hardness, strength, and toughness ($p < 0.05$). For elongation, the expected reduction in ductility was significant compared with the base alloy, but not between Hybrid-6, -8, and -10.

4.6 Wear Analysis

This research adopted a pin-on-disc tribometer to measure the wear behavior in terms of important parameters: wear rate, wear loss and coefficient of friction (COF). Test at constant speeds (100, 300, and 700 rpm), as well as tests at constant loads (10, 30, and 50 N), were carried out to represent the various service conditions. Addition of hard TiC particles and lubricating MoS_2 was done to minimize the loss of material and to increase the stability of surface and to decrease friction. The resultant data aids in determining the best reinforcement mix that provides the highest wear resistance and the composites are well suited to harsh usage in automotive, aerospace and structural parts.

At a constant speed, a monotonic improvement of wear performance Al2011-based hybrid composites reinforced with nano TiC and MoS_2 with increasing reinforcement content was observed. Wear rate (fig 13) indicated a significant decrease across all load levels, especially at the highest load (100 rpm - 50 N) where it decreased by 2.177 10^{-3} mm^3 /N m (0%) to 1.432 10^{-3} mm^3 /N m (10%), or about 34%. At 300 and 700 rpm, same reductions were noted which supported the effectiveness of reinforcement in losing a minimum amount of material. This trend was reflected in wear loss values (fig 14) which decreased at 100 rpm and 10 N to 0.265 mg, 0.118 mg and at 700 rpm and 50 N to 0.261 mg and 0.109 mg respectively proving increased wear resistance. The coefficient of friction (COF) (fig 15) has also been reduced, though the greatest reduction was at 100 rpm and 10 N where it fell to 0.397 as compared to 0.629. This results in the enhancement due to the hard load-bearing titanium carbide particles, which reduce abrasion on the surface and the lubricating effect of MoS_2 that forms tribo-film that reduces friction between the interface. Small inaccuracies can be explained by momentary effects of agglomeration, e.g. at 300 rpm and 30 N. On the whole, the results confirm the fact that the hybrid reinforcement system significantly enhances wear resistance and frictional stability under the different loading conditions at constant sliding speeds.

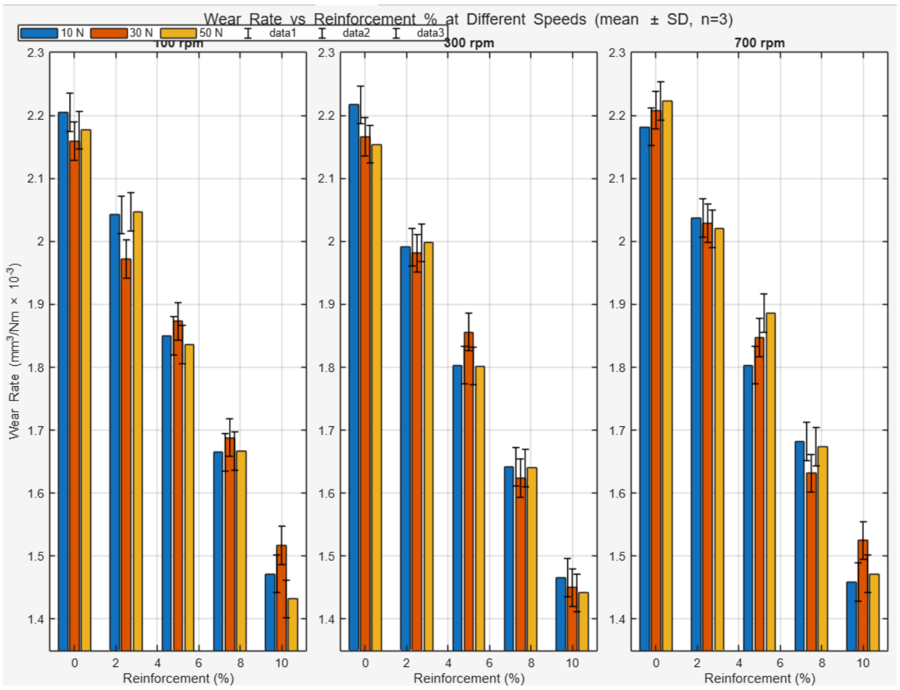

(a) (b) (c)

Fig. 13. (a) 100 rpm, (b) 300 rpm, (c) 700 rpm. Wear rate vs reinforcement percentage for loads 10/30/50 N. Mean ± SD (n = 3); error bars are ±1 SD

At constant loads, the nano TiC and MoS_2 reinforced Al2011 hybrid composites showed a significant enhancement of tribological performance at all test speeds (100, 300, and 700 rpm). The wear rate decreased steadily with elevated reinforcement, falling by ~33% at 100 rpm as the percentage of reinforcement varied between 0 (unreinforced alloy) and 10% at a fixed 10 N load (2.205 $10^{-3}mm^3/Nm$ to 1.472 $10^{-3}mm^3/Nm$ respectively). A similar trend was observed at 300 and 700rpm which showed increased wear resistance which is attributed to the combined effect of TiC and MoS_2. This pattern continued at greater loads (30 N and 50 N). E.g. the wear rate reduced at 50 N and 700 rpm to 1.472 $10^{-3}mm^3/Nm$ compared to 2.223, further confirming the robustness of the reinforcement subjected to harsh conditions. The value of wear loss also trended in a similar manner. Wear loss decreased by 0.265 mg (0) to 0.118 mg (10) at 10 N 100 rpm and 0.261 mg (0) to 0.109 mg (10) at 50 N 700 rpm. These consecutive decreases indicate how efficient reinforcement was in reducing material removal through load redistribution and inhibiting plastic flow and delamination.

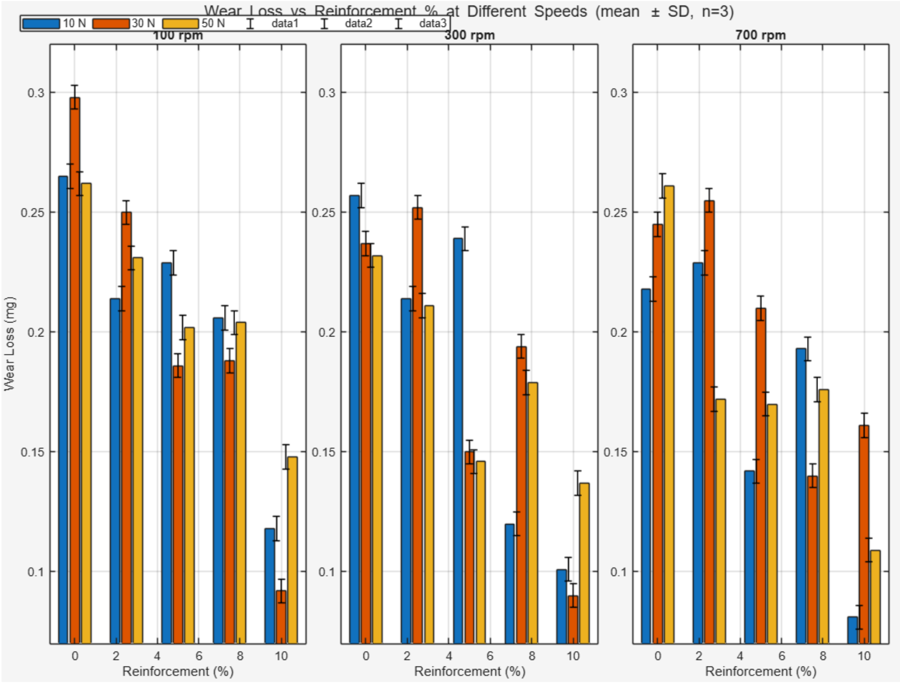

(a) (b) (c)

Fig. 14. (a) 100 rpm, (b) 300 rpm, (c) 700 rpm. Wear loss vs reinforcement percentage for loads 10/30/50 N. Mean ± SD (n = 3); error bars are ±1 SD

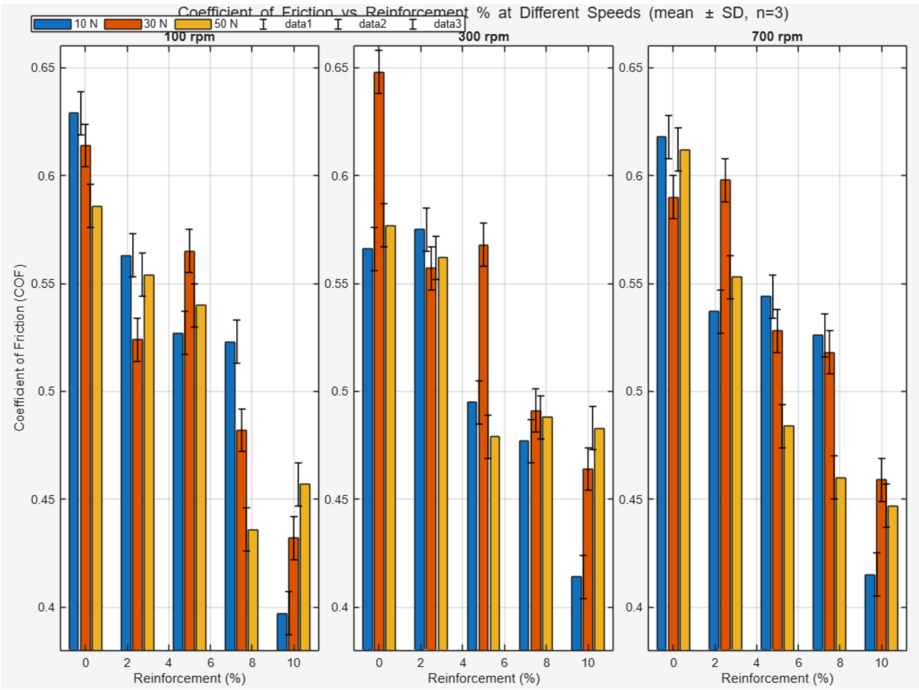

(a) (b) (c)

Fig. 15. (a) 100 rpm, (b) 300 rpm, (c) 700 rpm. COF vs reinforcement percentage for loads 10/30/50 N. Mean ± SD (n = 3); error bars are ±1 SD

The coefficient of friction (COF) also decreased steadily as the reinforcements were added. Initially at 10 N and 100 rpm the reduction in COF was 0.629 (0%) to 0.397 (10%) and this pattern followed at all other speeds and loads. MoS_2 played a leading role in enhancing this tendency through a lubricating film and TiC improved surface integrity reducing interfacial shear. These findings show evident changes in dominant wear mechanisms. Both the adhesive wear and abrasive wear caused severe damage to the unreinforced alloy, whereas the hybrid composites exhibited a less intense oxidative or boundary-lubricated wear regime attributed to the higher surface hardness value and a tribo-film generated by MoS_2. A combination of mechanical strengthening and tribological enhancement processes is the reason that limits wear behavior of Al2011-based hybrid composites reinforced with nano TiC and MoS_2. The first mechanism is the load bearing strength of the TiC nanoparticles which because of their high hardness and modulus strength, is prevented against plastic deformation and forms a barrier to ploughing and micro-cutting off the surface.

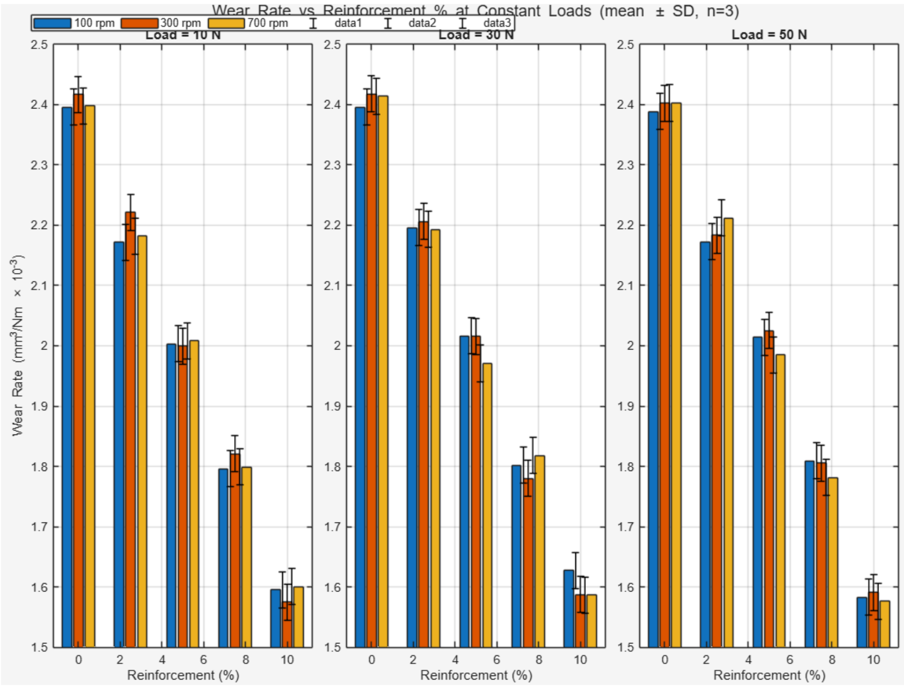

(a) (b) (c)

Fig. 16. (a) 10 N, (b) 30 N, (c) 50 N. Wear rate vs reinforcement percentage for speeds 100/300/700 rpm. Mean ± SD (n = 3); error bars are ±1 SD

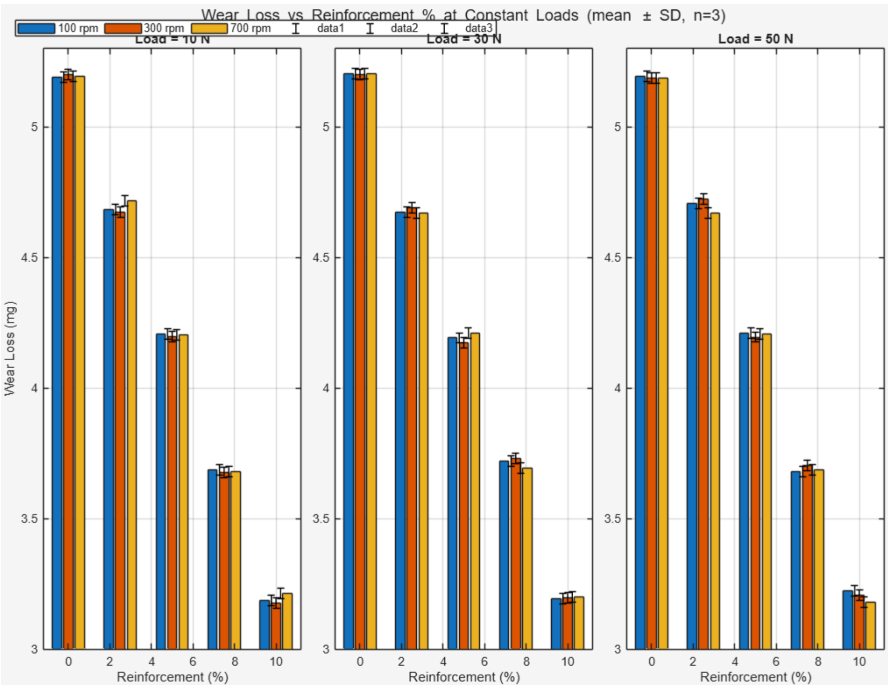

(a) (b) (c)

Fig. 17. (a) 10 N, (b) 30 N, (c) 50 N. Wear loss vs reinforcement percentage for speeds 100/300/700 rpm. Mean ± SD (n = 3); error bars are ±1 SD

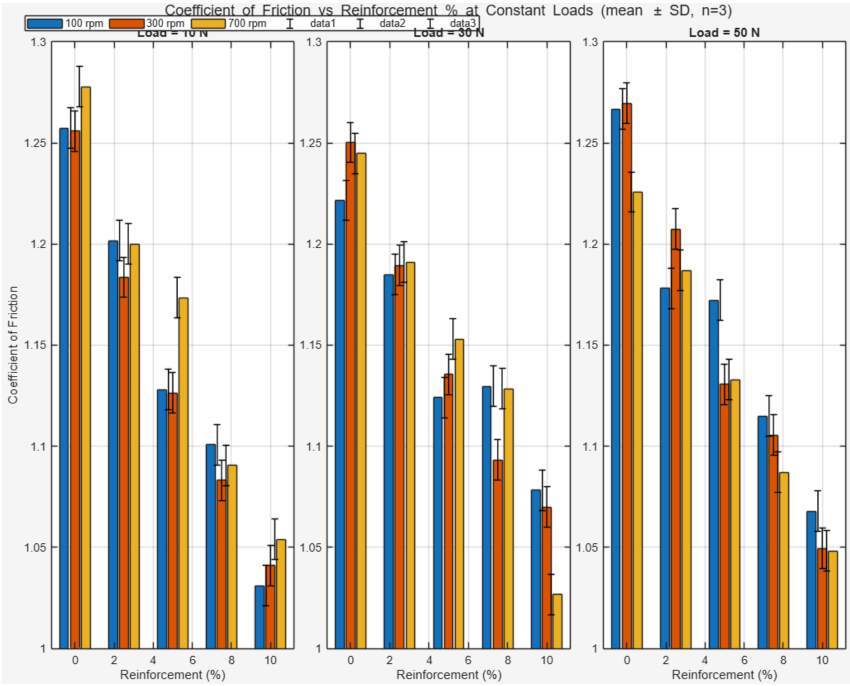

Fig. 18. (a) 10 N, (b) 30 N, (c) 50 N. COF vs reinforcement percentage for speeds 100/300/700 rpm. Mean ± SD (n = 3); error bars are ±1 SD

This results in a significant decrease of abrasive wear. At the same time, MoS_2, which also has a layered lamellar structure, is an important solid lubricant, providing a thin tribo-film with low shear strength at the sliding interface, which reduces interface shear stress, frictional heating, and adhesive wear. The synergistic effect of the combined wear contributions alters wear behavior shifting the limit of severe adhesive and abrasive wear common in the un-reinforced Al2011 alloy to a more stable oxidative and mild abrasive regime for the hybrid composites. Additionally, nano TiC also promotes grain refinement and Orowan strengthening via grains and surface hardening by thermal mismatch that led to better wear resistance and delamination inhibition. This improvement in wear rate, wear loss, and the coefficient of friction (COF) at all speeds and loads can therefore be explained by synergistic effect of reinforcement- induced hardening, interfacial film formation by MoS_2, and enhanced thermal stability. All these effects contribute to the enhanced ability of the composite to resist material removal and interfacial deterioration, particularly in dry sliding and under high-load conditions, which proves their potential to perform highly demanding tribological applications.

Table 4. One-way ANOVA results for tribological properties of Al2011–TiC–MoS_2 composites across all test conditions.

Property	F statistic	p-value	Significant (α=0.05)
Wear rate	204.49	9.57e-43	Yes
Wear loss	0.73	5.75e-01	No
COF	0.85	4.97e-01	No

It is vital to mention that the current wear tests were only carried out in dry sliding situations, which replicate extreme service conditions. Although it gives a consistent worst-case estimate of the performance of materials, most engineering applications like automotive engines, aircraft joints, and bearing systems are lubricated contacts or at a high temperature. Previous studies on Al-based nanocomposites have demonstrated that lubrication and temperature can have a significant effect on the shift between abrasive/adhesive wear and oxidative or delamination wear [23,24]. Therefore, current findings must be considered as minimum performance in severe conditions. The analysis will be extended to lubricated sliding and high-temperature environments in the future to develop a more comprehensive range of application of Al2011- TiC-MoS_2 alloys.

One-way ANOVA (Table 3) confirms a statistically significant composition effect for wear rate ($p < 0.001$). For wear loss and COF, the mean values decrease consistently with reinforcement, but the between-composition differences are not statistically significant at $\alpha = 0.05$ ($p > 0.05$). Therefore, these two responses are discussed in terms of practical magnitude of reduction rather than statistical significance. In addition to statistical significance, the magnitude of improvement is substantial. Compared with as-cast Al2011, the Hybrid-8 composite exhibited a ~13.4% increase in ultimate tensile strength, ~20% increase in hardness, and ~34% reduction in wear rate. These large effect sizes demonstrate the practical relevance of the optimized hybrid composition, even where statistical significance is limited by sample size. In addition to statistical significance, the magnitude of improvement is substantial. Compared with as-cast Al2011, the Hybrid-8 composite exhibited a ~13.4% increase in ultimate tensile strength, ~20% increase in hardness, and ~34% reduction in wear rate. These large effect sizes demonstrate the practical relevance of the optimized hybrid composition, even where statistical significance is limited by sample size. A schematic COF–time trace is included in Supplementary Fig. S1 to qualitatively illustrate run-in and steady-state behavior; continuous experimental COF time histories were not stored.

4.7 Microstructural Analysis of Worn Surfaces

SEM micrographs reveal solid demonstration of the wear behavior of the Al2011-based composites directly related to the composition of the reinforcement. The wear surface of the unreinforced Al2011 alloy is strongly degraded with deep grooves, ploughing marks, plastic deformation, and a large area of delamination.

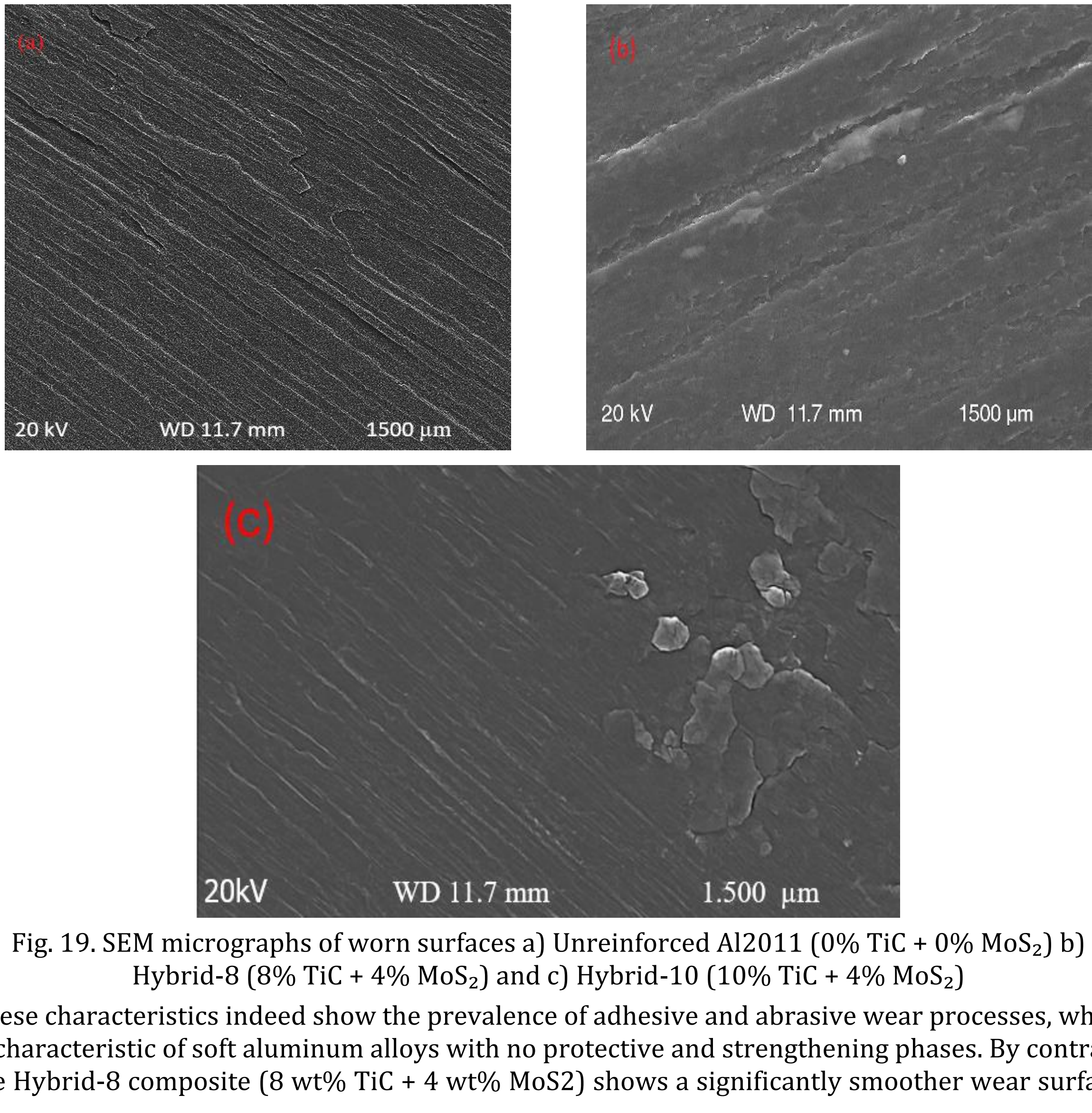

Fig. 19. SEM micrographs of worn surfaces a) Unreinforced Al2011 (0% TiC + 0% MoS_2) b) Hybrid-8 (8% TiC + 4% MoS_2) and c) Hybrid-10 (10% TiC + 4% MoS_2)

These characteristics indeed show the prevalence of adhesive and abrasive wear processes, which is characteristic of soft aluminum alloys with no protective and strengthening phases. By contrast, the Hybrid-8 composite (8 wt% TiC + 4 wt% MoS2) shows a significantly smoother wear surface, little deformation and evidence of a thin tribo film - hallmarks of a more stable oxidative and mild abrasive character. The TiC nanoparticles promote the matrix resistance to plastic flow and penetration, and MoS2 adds a low shear strength qualifying lubricating layer, which lowers frictional heat and adhesive interaction. The combination of the two leads to decreased wear rate, lower friction coefficient and improved surface integrity. The Hybrid-10 composite (10 wt% TiC + 4 wt% MoS2) however has a rougher morphology than Hybrid-8, showing evidence of reinforcement agglomeration, micro-cracking and pull-out of the particles. These characteristics are indicative of stress concentrations findings due to agglomeration and porosity, which eventually result in a decreased tribological performance. The comparison highlights the cruciality of the process of optimizing the reinforcement content: where Hybrid-8 manages to find the balance between hardening and lubrication, Hybrid-10 exceeds the limits where the process of reinforcement negatively affects the level of wear resistance as the highly processed content of reinforcement leads to flaws in the process and the occurrence of inhomogeneous areas. Complete ANOVA and Tukey HSD statistical summaries are provided in the Supplementary Information (Tables S1–S4).

5. Conclusion

The hybrid MMCs based on Al2011 reinforced with varying concentrations of nano Titanium Carbide (TiC) and constant concentrations of 4 wt% nano Molybdenum Disulfide (MoS_2) used in the present study were characterized and prepared by the stir casting technique.

- Addition of TiC resulted in tensile strength, hardness and impact toughness that were enhanced up to an optimum content value of 8 wt%, and with increasing contents, marginal degradation was experienced as a result of agglomeration and porosity.
- Even though MoS_2 did not produce a direct strength enhancement, friction reduction and enhanced interfacial bonding (which have a positive effect on tribological behaviour) were also observed.
- Wear testing indicated that the wear rate, wear loss and coefficient of friction reduced considerably with increasing reinforcement particularly under constant speed and load conditions.
- Hybrid-8 composition (8% TiC + 4% MoS_2) turned out to be the most optimal one, as it offers the best strength, ductility, and wear resistance.
- SEM of worn surfaces gave evidence to smoother surfaces and formation of tribo-films in Hybrid-8 but showed clusters and micro-cracks in Hybrid-10.
- The superiority of the Hybrid-8 composition was statistically validated using ANOVA, which confirmed significant improvements in hardness, strength, toughness, and tribological properties compared with neighboring compositions.

5.1 Engineering Implications

The Al2011-TiC- MoS_2 hybrid composites optimized exhibit great potential in automotive engine components, aerospace fittings, bearings, and tooling applications, which demand high strength and low wear. The stir casting route is also scalable and this adds even more relevance to industry.

5.2 Limitations and Future Research

The current research was restricted to SEM-based characterization and dry sliding wear experiments. EBSD /TEM analyses should also be conducted in future to measure the grain size distribution and dislocation density to have a better interpretation of Hall Petch and Orowan strengthening. Moreover, high-temperature and lubricated wear tests will also be required to approximate real-life use and verify its usability in commerce.

References

[1] Surappa MK. Aluminium matrix composites: Challenges and opportunities. Sādhanā. 2003;28(1-2):319-334. https://doi.org/10.1007/BF02717141

[2] Li J, et al. The tribological properties of nano-lubricants and their application on bearings: Recent research progress. Int J Adv Manuf Technol. 2024;134:3051-3082. https://doi.org/10.1007/s00170-024-14351-8

[3] Bhane AB, Ramani HB. Mechanical and tribological properties of nano composites under dry sliding conditions: A study and investigation. Int J Mech Eng. 2022;7(10):137-144.

[4] Sethi AK, et al. Fabrication and evaluation of aluminum hybrid metal matrix composite via powder metallurgy approach. J Polymer and Composites. 2024;12(2):205-211.

[5] Teja VS, Sastry KSBSVS, Srinivas BNV, Krishnaji KV. Characterization of Cu-SiC-Gr hybrid metal matrix composite. Int J Adv Mech Therm Eng. 2019.

[6] Singhal V, et al. Study of the influence of nanoparticle reinforcement on the mechanical and tribological performance of aluminum matrix composites-A review. Lubricants. 2025;13(2):93. https://doi.org/10.3390/lubricants13020093

[7] Narayanasamy P, et al. Effect of hybridizing MoS_2 on the tribological behaviour of Mg-TiC composites. Trans Indian Inst Met. 2015. https://doi.org/10.1007/s12666-015-0530-z

[8] Mao H, et al. Microstructure, mechanical properties, and reinforcement mechanism of second-phase reinforced TiC-based composites: A review. Coatings. 2022. https://doi.org/10.3390/coatings12060801

[9] Malek A. Review of stir casting technique and technical challenges for ceramic reinforcement particulate and aluminium matrix composites. Építőanyag - J Silicate Based and Composite Materials. 2020;72(6):190-197. https://doi.org/10.14382/epitoanyag-jsbcm.2020.32

[10] Bhanodaya KBN. Comprehensive analysis of stir casting process of aluminum-based composites with silicon carbide reinforcements. NanoWorld J. 2023;9(Suppl 4):S257-S261. https://doi.org/10.17756/nwj.2023-s4-044

[11] Dhulipalla A, et al. Synthesis and machining characteristics of novel TiC ceramic and MoS_2 soft particulate reinforced aluminium alloy 7075 matrix composites. Manufacturing Lett. 2020;24:82-86. https://doi.org/10.1016/j.mfglet.2020.04.001

[12] Umanath K, et al. Optimization of wear properties on AA7075/SiC/MoS_2 hybrid composites. Mater Today: Proc. 2021.

[13] Gopalakrishnan R, et al. Influence of MoS_2 with TiC on the tribological and wear properties of hybrid aluminum composites (AA7075). In: Advances in Materials and Manufacturing. 2023. https://doi.org/10.1007/978-981-19-8497-6_27

[14] Suchendra KR, Sreenivasa RM. Microstructure, mechanical and fracture behavior of Al_2O_3-MoS_2 reinforced Al6061 hybrid composite. Frattura ed Integrità Strutturale. 2022. https://doi.org/10.3221/IGF-ESIS.61.16

[15] Sidharthan S, et al. Mechanical property analysis and tribological response optimization of SiC and MoS_2 reinforced hybrid aluminum functionally graded composite through Taguchi's DOE. J Manuf Process. 2023;102:965-984. https://doi.org/10.1016/j.jmapro.2023.08.013

[16] Sharma SK, et al. Progress in aluminum-based composites prepared by stir casting: Mechanical and tribological properties for automotive, aerospace, and military applications. Lubricants. 2024;12:421. https://doi.org/10.3390/lubricants12120421

[17] Sharath BN, et al. Enhancing tribological performance: A review of ceramic-reinforced aluminum hybrid composites. Tribology Int Reports. 2023. https://doi.org/10.1016/j.hybadv.2023.100094

[18] Hemadri K, et al. Investigation on mechanical characterization of Al/MoS_2/WC hybrid composite. Mater Today: Proc. 2022. https://doi.org/10.1016/j.matpr.2022.08.014

[19] Zhao D, et al. Influence of TiC particle size on microstructural evolution and fracture mechanism of TiC/Al-Cu composites. J Alloys Compd. 2024;1008:176763. https://doi.org/10.1016/j.jallcom.2024.176763

[20] Carneiro Í, Simões S. Recent advances in EBSD characterization of metals. Metals. 2020;10:1097. https://doi.org/10.3390/met10081097

[21] Zheng JH, et al. Quantifying geometrically necessary dislocation density during hot deformation in AA6082 Al alloy. Mater Sci Eng A. 2021;814. https://doi.org/10.1016/j.msea.2021.141158